

A reusable surface-quaternized nanocellulose-based hybrid cryogel loaded with N-doped TiO₂ for self-integrated adsorption/photo-degradation of methyl orange dye

Yufei Chen^a, Hongzhi Liu^{a,b*}, Biyao Geng^a, Jing Ru^a, Chen Cheng^a, Likui Wang^{c*}

^aSchool of Engineering, Zhejiang Agriculture and Forestry University, Lin'an, Hangzhou, Zhejiang Province, 311300, China.

^bNational Engineering and Technology Research Center of Wood-based Resources Comprehensive Utilization, Lin'an, Hangzhou, Zhejiang Province, 311300, China.

^cSchool of Chemical and Materials Engineering, Jiangnan University, Wuxi, Jiangsu Province, 214122, China.

* Corresponding author: Email: hzliu@iccas.ac.cn (H. Liu); lkwang@jiangnan.edu.cn (L. Wang).

SUPPORTING INFORMATION

Supporting Tables and Figures

Table S1 BET specific surface area values and porous characteristics of the Q-NFC based cryogels

Samples	S_{BET} (m²/g)	Total pore volume (cm³·g⁻¹)	Average pore diameter (nm)
Q-NFC	24.31	0.041	14.67
10N-NFC	19.54	0.037	12.15
10Ti-NFC	16.12	0.028	11.17
10N10Ti-NFC	17.42	0.032	12.01

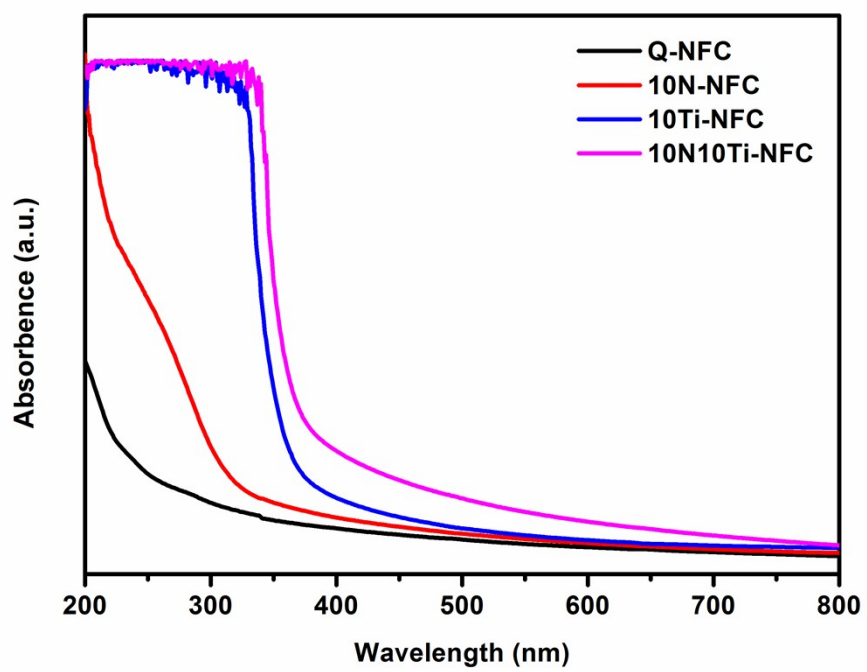


Figure S1. UV-Visible absorption spectra for the Q-NFC and Q-NFC based cryogels.

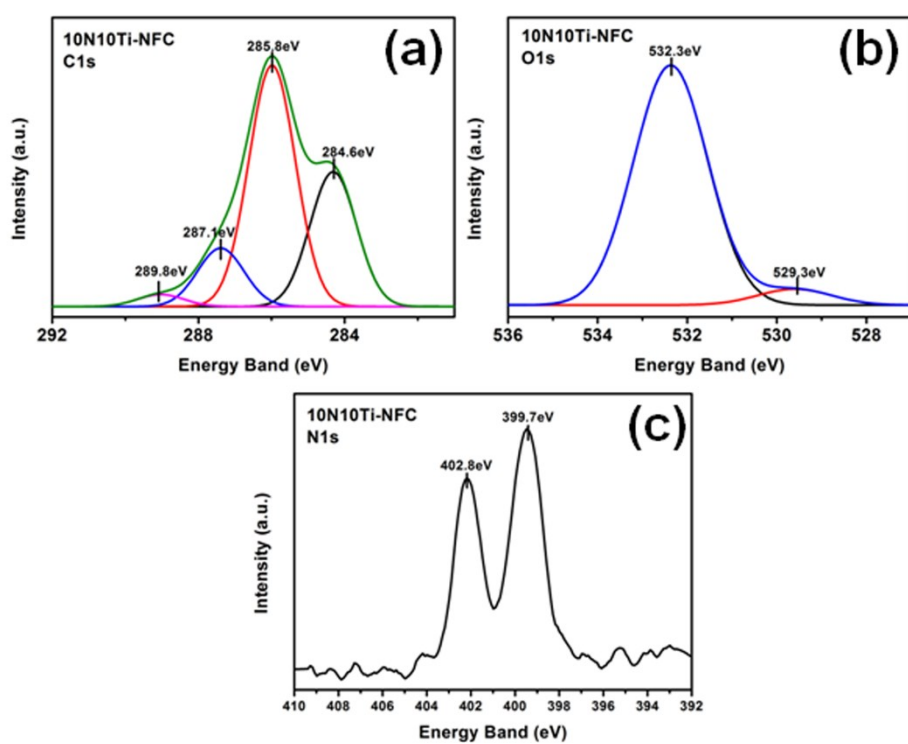


Figure S2. C1s (a), O1s (b) and N1s (c) XPS spectra of the 10N10Ti-NFC cryogel.

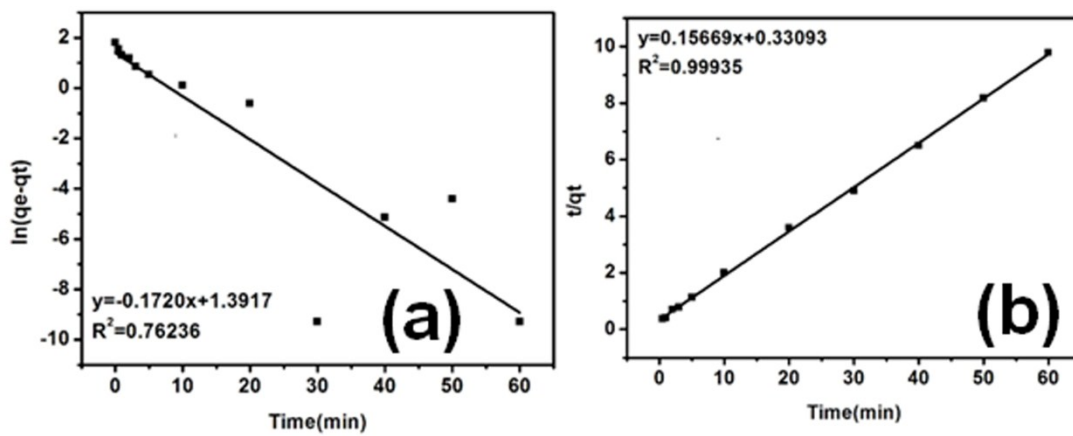


Figure S3. Fitting curves of MO adsorption data with pseudo-first-order model (a) and pseudo-second-order model (b) for 10N10Ti-NFC cryogel, respectively.

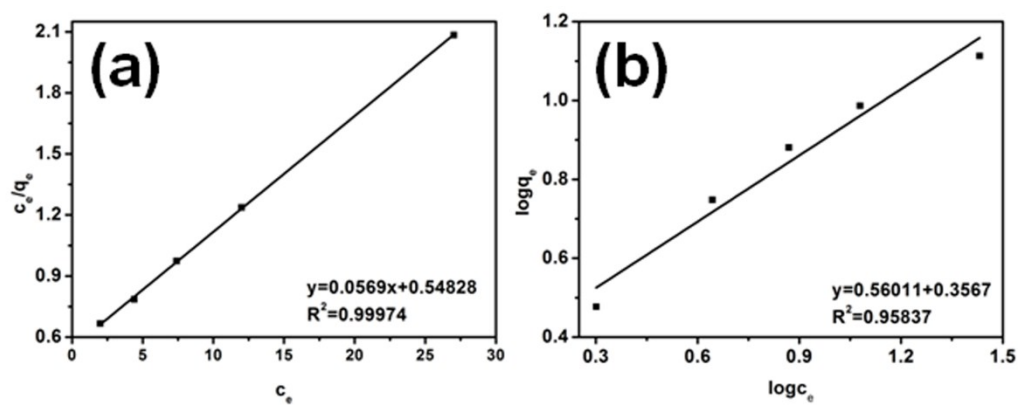


Figure S4. Isotherm plots of Langmuir (a) and Freundlich (b) for the adsorption of MO on 10N10Ti-NFC (1 g L⁻¹) at 20°C (Note: the initial concentrations of MO were 5, 10, 15, 20 and 40 mg·L⁻¹).

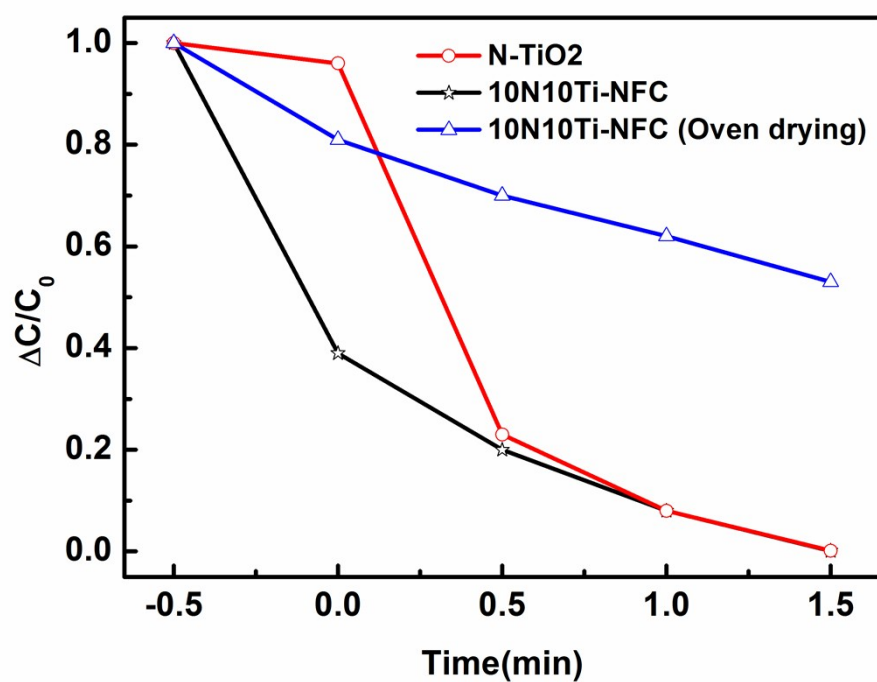


Figure S5. The photo-degradation performance of the N-TiO₂, 10N10Ti-NFC (freeze drying) and 10N10Ti-NFC (oven drying) under the irradiation of simulated solar light.

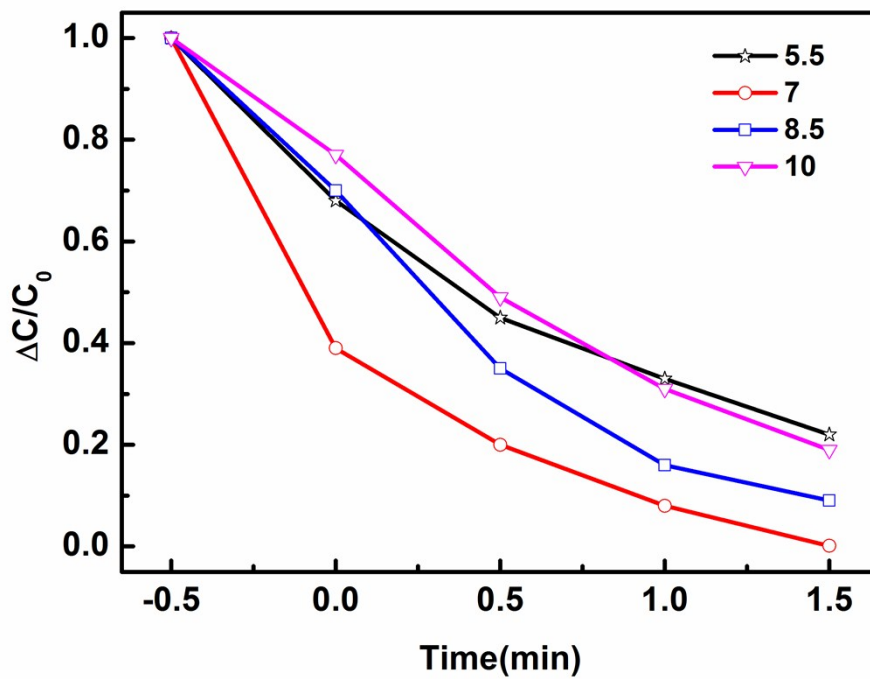


Figure S6. Effect of pH value on photo-degradation performance of 10N10Ti-NFC.